Genomics xxx (xxxx) xxx–xxx

Contents lists available at ScienceDirect

Genomics

journal homepage: www.elsevier.com/locate/ygeno

Alternative metabolic routes in channeling xylose to cordycepin production of *Cordyceps militaris* identified by comparative transcriptome analysis

Boontariga Wongsa[a], Nachon Raethong[b], Pramote Chumnanpuen[a,c], Jirasak Wong-ekkabut[c,d], Kobkul Laoteng[e,*], Wanwipa Vongsangnak[a,f,**]

[a] Department of Zoology, Faculty of Science, Kasetsart University, Bangkok 10900, Thailand
[b] Interdisciplinary Graduate Program in Bioscience, Faculty of Science, Kasetsart University, Bangkok 10900, Thailand
[c] Computational Biomodelling Laboratory for Agricultural Science and Technology (CBLAST), Faculty of Science, Kasetsart University, Bangkok 10900, Thailand
[d] Department of Physics, Faculty of Science, Kasetsart University, Bangkok 10900, Thailand
[e] Functional Ingredients and Food Innovation Research Group, National Center for Genetic Engineering and Biotechnology (BIOTEC), National Science and Technology Development Agency (NSTDA), Pathum Thani 12120, Thailand
[f] Omics Center for Agriculture, Bioresources, Food, and Health, Faculty of Science, Kasetsart University (OmiKU), Bangkok 10900, Thailand

ARTICLE INFO

Keywords:
Cordyceps militaris
Cordycepin
Carbon sources
Metabolic routes
Transcriptome analysis

ABSTRACT

The responsive mechanism of *C. militaris* TBRC7358 on xylose utilization was investigated by comparative analysis of transcriptomes, growth kinetics and cordycepin productions. The result showed that the culture grown on xylose exhibited high production yield of cordycepin on dry biomass. Comparing xylose to other carbon sources, a set of significantly up-regulated genes in xylose were enriched in pentose and glucuronate interconversion, and cordycepin biosynthesis. After validating up-regulated genes using quantitative real-time PCR, interestingly, putative alternative 3′-AMP-associated metabolic route on cordycepin biosynthesis was identified. Through reporter metabolites analysis of *C. militaris*, significant metabolites (e.g., AMP, glycine and L-glutamate) were identified guiding involvement of growth and cordycepin production. These findings suggested that there was a cooperative mechanism in transcriptional control of the supplying precursors pool directed towards the cordycepin biosynthesis through main and putative alternative metabolic routes for leverage of cell growth and cordycepin production on xylose of *C. militaris* strain TBRC7358.

1. Introduction

Cordyceps represents a large genus of entomopathogenic fungi, in which several species have a long history of applications in agriculture and biotechnological industries. In Asia, *Cordyceps militaris* belonging to the family Cordycipitaceae is being used as traditional Chinese medicine and functional ingredient in health foods and cosmetics [1,2]. In addition to natural growing on arthropods, the progress in artificial cultivation of this fungus has driven its exploitation for biomanufacturing of certain valuable metabolites [3]. Many attempts have been done to develop the efficient cultivation process for improving the mycelial biomass and cordycepin production by *C. militaris*. For medium optimization, the effects of carbon, nitrogen, and mineral sources on cell growth and cordycepin production were studied by surface liquid cultivation [4–6]. Among them, a carbon source is one of biotic factors, which has been investigated in the context of metabolic regulation in *C. militaris* for further translating to industrial practices. It has been reported that glucose (C6) is an optimal carbon source for *C. militaris* cultivation as the result of specific growth and sugar consumption rates [7]. The sucrose (i.e. disaccharide sugar, C12) has been uncovered as an inducer for cordycepin production [8] and practically used as a cheap substrate for large-scale cultivation of *C. militaris* [9]. Moreover, the xylose (i.e. pentose sugar, C5) could be used as an alternative carbon source for cordycepin production, which the production yield was comparable to the glucose and sucrose cultures [8]. However, the channeling of various carbon sources towards cordycepin production of *C. militaris* remains largely unexplored.

The available *C. militaris* CM01 genome [10] and the accessible *C. militaris* TBRC6039 RNA-sequencing data [8] as well as the emerging computer-assisted tools currently permit the data integration for dissecting cellular metabolism underlying cordycepin production [11]. Generally, cordycepin (3′-deoxyadenosine) is generated from the main

* Corresponding author.
** Corresponding author at: Department of Zoology, Faculty of Science, Kasetsart University, Bangkok 10900, Thailand.
E-mail addresses: kobkul@biotec.or.th (K. Laoteng), wanwipa.v@ku.ac.th (W. Vongsangnak).

https://doi.org/10.1016/j.ygeno.2019.04.015
Received 21 January 2019; Received in revised form 14 April 2019; Accepted 21 April 2019

precursor, adenosine and adenine through the stepwise reactions catalyzed by purine-nucleoside phosphorylase (EC: 2.4.2.1) via nucleotide metabolism [11]. Alternatively, the AMP [11] and 3′-AMP [12] might be precursors for cordycepin production. The discrimination in metabolic routes governing the cordycepin biosynthesis among different strains of *C. militaris*, particularly in terms of metabolic responses to carbon sources have not been addressed. In this study, we therefore emphasized on the transcriptional response of the *C. militaris* strain TBRC7358 to xylose utilization for cordycepin biosynthesis. By pairwise comparative analysis of transcriptomes derived from the xylose versus glucose cultures, and xylose versus sucrose cultures, the informative data relevant to the energy and precursor supply for cell growth and cordycepin biosynthesis were elaborated from differential expressed genes (DEGs) and reporter metabolites analysis. In addition, the transcriptome analysis of two strains of *C. militaris*, TBRC7358 and TBRC6039 were also subjected for identifying alternative metabolic routes involved in cordycepin biosynthesis, in particular when xylose was used as a sole carbon source. For further validating the transcriptome data, gene expression analysis using quantitative real-time PCR analysis (qRT-PCR) was carried out. This study provides an insight into molecular mechanism underlying key metabolic routes in channeling xylose to cordycepin production of *C. militaris* strain TBRC7358.

2. Results and discussion

2.1. Phenotypic characteristics of C. militaris strain TBRC7358 using different carbon sources

Using different carbon sources for cultivations of *C. miliaris* strain TBRC7358, the profiles of cell growth and sugar consumption at different time courses are shown in Fig. 1. Among carbon sources tested, sucrose and glucose were most favorable for growth, which provided maximum biomass and specific growth rates (μ_{max}) at similar values (0.18–0.19 day^{-1}) (Table 1). In contrast, a slow growth rate was found in the xylose culture (0.09 ± 0.01 day^{-1}).These results are in agreement with the previous reports of other strains of *C. militaris* [8,13]. Considering the cordycepin production, the maximum cordycepin titer (249.74 ± 12.71 mg/L) was observed in the glucose culture, which the production yield ($Y_{p/s}$) was 0.026 ± 0.001 g/g, even though its biomass was slightly lower than the sucrose culture. Interestingly, there was no much difference in the production yield of cordycepin ($Y_{p/s}$) between the glucose (0.026 ± 0.001 g/g) and xylose cultures (0.024 ± 0.001 g/g) of *C. militaris*. However, the xylose culture showed the highest yield of extracellular cordycepin on dry biomass (0.094 ± 0.002 g /g), although it was a poor carbon source for cell growth (Table 1). These results are coincided with the previous report of the constructed metabolic network of *C. militaris* [11], guiding that xylose might be a favorable sugar for cordycepin production according to its role as a structural precursor directed towards cordycepin formation. Promisingly, xylose could be used as an alternative carbon source if the cordycepin is a desired extracellular metabolite product, not the whole-cell mass product. As such, the exploitation of renewable sources from biorefinery process, particularly the lignocellulosic sugars consisting of glucose and xylose, as well as agroindustrial by-products might be a prospect for development of economically feasible process for cordycepin production by *C. militaris*. We postulated that the improved production of cordycepin-rich biomass on xylose is a challenge in value addition of the fungal product for particular applications. Obviously, the strain TBRC7358 produced higher cordycepin titer (235.39 ± 5.17 mg/L) (Table 1) than the reference strain TBRC6039 (149.50 ± 15.71 mg/L) [8], even though biomass productivities of both strains were similarly observed in xylose culture (0.06–0.07 g/L/day) (see Table 1 and [8]). Indeed, better understanding of the role of xylose on biomass and cordycepin production at systems level is required for further improving either the fungal strain or the production process. Besides, the effect of the addition of xylose into the medium containing the other carbon sources as dual sugars might be further investigated for improving the cordycepin production.

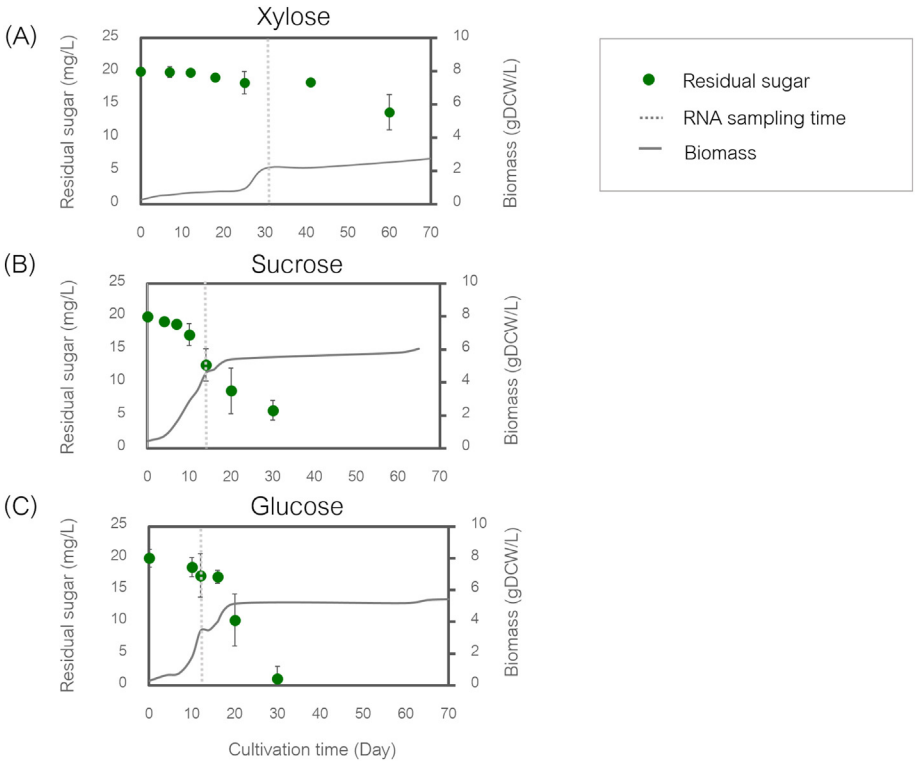

Fig. 1. The fermentation profiles of *C. militaris* strain TBRC7358 in defined medium containing individual carbon source. All cultivations were performed in independently triplicates. RNA samples were extracted from the 12-, 14- and 30-day cultures grown on glucose, sucrose, and xylose, respectively.

Table 1
Growth characteristics of *C. militaris* strain TBRC7358 using different carbon sources.

Characteristics	Xylose	Sucrose	Glucose
Maximum specific growth rates (μ_{max}, day^{-1})	0.09 ± 0.01[b]	0.19 ± 0.02[a]	0.18 ± 0.01[a]
*Biomass productivity (g/L/day)	0.07 ± 0.01[b]	0.35 ± 0.05[a]	0.30 ± 0.03[a]
**Extracellular cordycepin titer (mg/L)	235.39 ± 5.17[a,b]	212.70 ± 5.93[b]	249.74 ± 12.71[a]
**Extracellular cordycepin productivity (mg/L/day)	3.92 ± 0.09[c]	10.64 ± 0.30[b]	12.49 ± 0.64[a]
**r_{sugar}(mmol g/DCW/day)	0.44 ± 0.03[a]	0.3 ± 0.09[a]	0.53 ± 0.22[a]
**$Y_{x/s}$ (g DCW/g sugar)	0.25 ± 0.02[a]	0.52 ± 0.18[a]	0.6 ± 0.27[a]
**$Y_{p/s}$ (g extracellular cordycepin/g sugar)	0.024 ± 0.001[a]	0.019 ± 0.001[b]	0.026 ± 0.001[a]
**$Y_{p/x}$ (g extracellular cordycepin/ g DCW)	0.094 ± 0.002[a]	0.039 ± 0.001[c]	0.049 ± 0.002[b]

Note: Values are mean ± SD ($n = 3$).
a,b,c Different upper-case letters in rows indicate statistically significant differences ($P \leq .05$, Tukey's test).
* Biomass productivities were obtained from of the glucose, sucrose and xylose cultures grown for 12, 14 and 30 days, respectively.
** Cordycepin productivities were obtained from the glucose, sucrose and xylose cultures grown for 20, 20 and 60 days, respectively.

2.2. Differential expression of *C. militaris* genes in response to xylose utilization

To investigate DEGs of the xylose culture of *C. militaris* strain TBRC7358 as compared to the cultures using other carbon sources, the mRNAs pools derived from the xylose, sucrose and glucose cultures were subjected for sequencing. As a result, total raw reads in an average of 50.53 Megabase pairs (Mb) were gained. After filtered adaptors and ambiguous reads, total clean reads were finally retrieved with an average of 44.99 Mb with sequencing quality of 98.66%, 98.63% and 98.65% for xylose, sucrose, and glucose cultures, respectively as summarized in Table 2. Through Trinity-assembling pipeline, it resulted in a total of 16,566 transcripts with the total length of 28.90 Mb and GC content of 55.81%. Of 16,566 transcripts (Table 2), a total of 15,625 transcripts with the threshold of FPKM ≥1 were identified, and 13,391 transcripts (Table 2, Supplementary file 1) were then assigned as protein-encoding genes based on functional annotation analysis (see Materials and Methods). The results of genes with differential expression analysis (FDR ≤ 0.001) showed that a total of 3645 significantly DEGs was found across the xylose, sucrose and glucose cultures (Fig. 2). When compared between a pair of the cultures, the differential expressions of 1785 and 2734 genes were observed in the xylose versus glucose cultures, and the xylose versus sucrose cultures, respectively (Fig. 2 and see Supplementary file 2). Among the 13,391 transcripts, besides the identified 3645 significantly DEGs, it was also found that putative 3631 genes encoding functional proteins which were annotated based on KEGG database [14] and thus classified into four main function categories, including metabolism, environmental information processing, genetic information processing and cellular process as illustrated in Fig. 3. Interestingly, there were 2699 genes (74.3% of the total annotated genes) involved in the cellular metabolism (Supplementary file 3), which were the largest category found in the protein functions of *C. militaris*, whereas the smallest category of genes involved in environmental information processing (99 genes). Of 2699 genes identified in the fungal strain TBRC7358, a number of genes was highly enriched in carbohydrate metabolism (1077 genes) followed by amino acid metabolism (590 genes), lipid metabolism (294 genes), nucleotide metabolism (212 genes), metabolism of cofactors and vitamins (162 genes), energy metabolism (149 genes), metabolism of other amino acids (96 genes), glycan biosynthesis and metabolism (88 genes), secondary metabolites biosynthesis (19 genes) and metabolism of terpenoids and polyketides (12 genes) as shown in Fig. 3. This result is coincided with the functional annotation of the expressed genes identified in another strain of *C. militaris* [8].

Considering the protein-encoding genes in metabolism category, up-regulation of 53 DEGs were identified in the xylose culture by pairwise comparisons with those of the glucose or sucrose cultures (see Supplementary file 4). Of these, 28 genes with high expression values (≥1.5 average in log2 fold change) were distributed into 21 sub-functional categories as listed in Table 3 and Supplementary file 4. As expected, we found the largest number of DEGs involved in pentose and glucuronate interconversion of *C. militaris* TBRC7358, for examples D-xylulose reductase (EC: 1.1.1.9), D-xylulokinase (EC: 2.7.1.17), and glyceraldehyde reductase (EC: 1.1.1.372) (Table 3). In addition, we also found a number of DEGs involved in fructose and mannose metabolism, such as L-rhamnose 1-dehydrogenase (EC: 1.1.1.173), sorbose reductase (EC: 1.1.1.289) and sorbitol dehydrogenase (EC: 1.1.1.14). As such, it seems likely that *C. militaris* strain TBRC7358 might be capable of utilizing a wide range of carbon sources, such as glycerol [15], arabinose [16], rhamnofuranose [17] and sorbose [18] in addition to the carbon sources tested in this study.

2.3. Identifying possible metabolic routes participated in precursor supply for cordycepin biosynthesis in *C. militaris*

It is well recognized that adenine metabolic pathway plays a key role in cordycepin biosynthesis of *C. militaris*. Various forms of adenine (AMP, ADP, and ATP) could be used as the precursors for cordycepin formation as previously described [19,20]. It has been reported that the adenine metabolic pathway towards putative cordycepin biosynthesis contained 31 genes, 21 enzymes, and 25 biochemical reactions guided by the constructed metabolic network of *C. militaris* [11] Accordingly, the transcriptome data of *C. militaris* strain TBRC7358 grown at different carbon sources were then integrated into the constructed metabolic network of *C. militaris* by using reporter metabolites analysis [21]. Expectedly, the top 25 significant metabolites were found in relation to the cell growth and cordycepin production of the xylose cultures when compared with the glucose or sucrose cultures (Supplementary file 5). The finding of the reporter metabolites (e.g. 2-oxoglutarate, acetyl-CoA, coenzyme A, pyruvate, $NADP^+$, NADPH, D-fructose 6-phosphate, alpha-D-glucose 6-phosphate, AMP, ADP and ATP) could simply explain their involvements in currency of biological life in contexts of precursor supply, energy and redox metabolisms for cell growth.

Among these reporter metabolites, the integrative analysis showed that AMP was the most significant metabolite based on the highest number of neighbors and high *Z*-score. As shown in Fig. 4, the AMP might be directed to cordycepin biosynthetic pathway [10,22] in addition to the function in other metabolisms of the fungal cell [23]. Furthermore, this analysis also captured the other metabolites related to formation of amino acids (i.e. glycine [24] and L-glutamate), which might be used as precursor pools for cordycepin biosynthesis. The result of reporter metabolites analysis suggests that the hidden metabolic routes associated with the supply of precursors for cordycepin biosynthesis were probably active when using the particular carbon source for the fungal cultivation, e.g., changing from glucose to xylose or sucrose to xylose (Fig. 4). Thus, the up-regulated expression of the genes in metabolic routes governing the precursor formation and channeling the precursor towards cordycepin biosynthesis could describe the

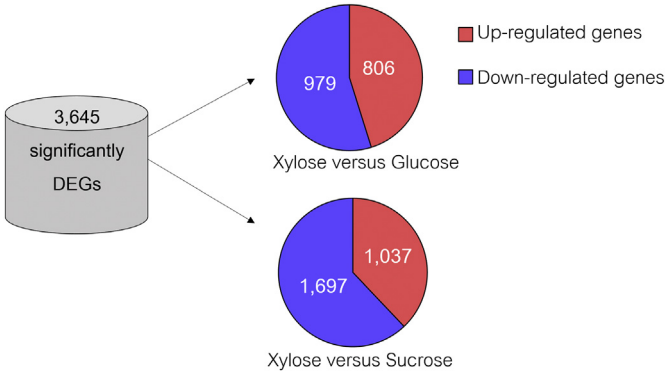

Fig. 2. The number of significantly DEGs of *C. militaris* strain TBRC7358 across pairwise carbon sources comparisons. Statistical significance of DEGs under FDR ≤ 0.001.

fungal cell physiology in xylose cultivation, which exhibited high extracellular cordycepin yield on dry biomass (Table 1), which is in consistent with the previous report of the strain TBRC6039 [8]. Possibly, there was a cooperation in controlling metabolic routes through transcription level for leverage of cell growth and cordycepin production on xylose of *C. militaris*.

2.4. Identifying putative alternative routes towards 3′-AMP-associated cordycepin biosynthesis

Comparative analysis of the transcriptomes between two strains, TBRC7358 and TBRC6039, showed a difference in expression levels of a set of genes in the xylose cultivation. Two genes (i.e. Unigene8329 and Unigene6827) encoding for 2′,3′-cyclic-nucleotide 2′-phosphodiesterase (EC: 3.1.4.16), which catalyze the conversion of 2′,3′-cAMP to 3′-AMP [25], were up-regulated in the strain TBRC7358 (Fig. 5 and Table 4). This indicates that expression of these particular genes was also dependent on the strain of *C. militaris* in addition to the carbon source utilized.

Gathering the results, it was also indicated that the cordycepin biosynthetic pathway in the *C. militaris* TBRC7358 was highly associated with the 3′-AMP formation as presented in Fig. 5 and Table 4. This finding is in agreement with the previous study by Xia et al. (2017) [12], postulating that the cordycepin precursor (3′-AMP) can be synthesized from 2′,3′-cyclic AMP, which is a by-product from mRNA degradation [12,26] of *C. militaris*. Further, we searched the other up-regulated genes in *C. militaris* strain TBRC7358, which are responsible for the formation of 2′,3′-cyclic AMP. As listed in Table 4, interestingly, Unigene902 encoding for CCA tRNA nucleotidyltransferase (EC: 2.7.7.72) [27] was found in the strain TBRC7358, as a significantly up-regulated expression with a fold change of 2.82. In the cordycepin biosynthetic pathway, 2′-carbonyl-3′-deoxyadenosine (2C3DA) is an intermediate precursor derived from 3′-AMP. Expectedly, we found the up-regulation of Unigene5711 with a fold change of 1.9 in the strain TBRC7358 (Table 4), which encoded the oxidoreductase domain-containing protein responsible for the conversion of 2C3DA to cordycepin. As summarized in Fig. 5, we thus propose the existence of putative alternative 3′-AMP-associated route in cordycepin biosynthesis of *C. militaris*. Through 2′,3′-cyclic AMP and 2C3DA, the association of metabolic functions for cordycepin formation might be active accordingly, in particular for the xylose culture of *C. militaris* strain TBRC7358. These might further improve cordycepin production in *C. militaris*.

Apart from the putative alternative route as above mentioned, the main metabolic routes for cordycepin biosynthesis in both strains of *C. militaris* were also focused. As expected, a set of up-regulated genes were identified in the xylose culture of the strain TBRC7358, which involved in the metabolic reactions of adenosine via 3′-AMP formation towards cordycepin biosynthesis [8,11,12], such as adenylosuccinate synthase (EC: 6.3.4.4, Unigene2635), adenylosuccinate lyase (EC: 4.3.2.2, Unigene5434), ATP phosphoribosyltransferase (EC: 2.4.2.17, Unigene6275; CL2354.Contig2; CL2354.Contig1), oxidoreductase domain-containing protein (Unigene5711) (Fig. 5 and Table 4). Additionally, we also found the up-regulated genes involved in adenylate kinase (EC: 2.7.4.3, CL794.Contig3), adenosine kinase (EC: 2.7.1.20, CL1742.Contig2), and nucleoside-diphosphate kinase (EC: 2.7.4.6, Unigene1364) as shown in Table 4.

Table 2
Transcriptome statistics of *C. militaris* strain TBRC7358.

Features	Sucrose	Glucose	Xylose
Total raw reads (Mb)	49.78	52.04	49.78
Total clean reads (Mb)	44.77	45.81	44.41
Sequencing quality (%)	98.63	98.65	98.66
Number of transcripts	17,069	16,184	15,562
Total number of transcripts	16,566		
(Total number of protein-encoding genes)	(13,391)		

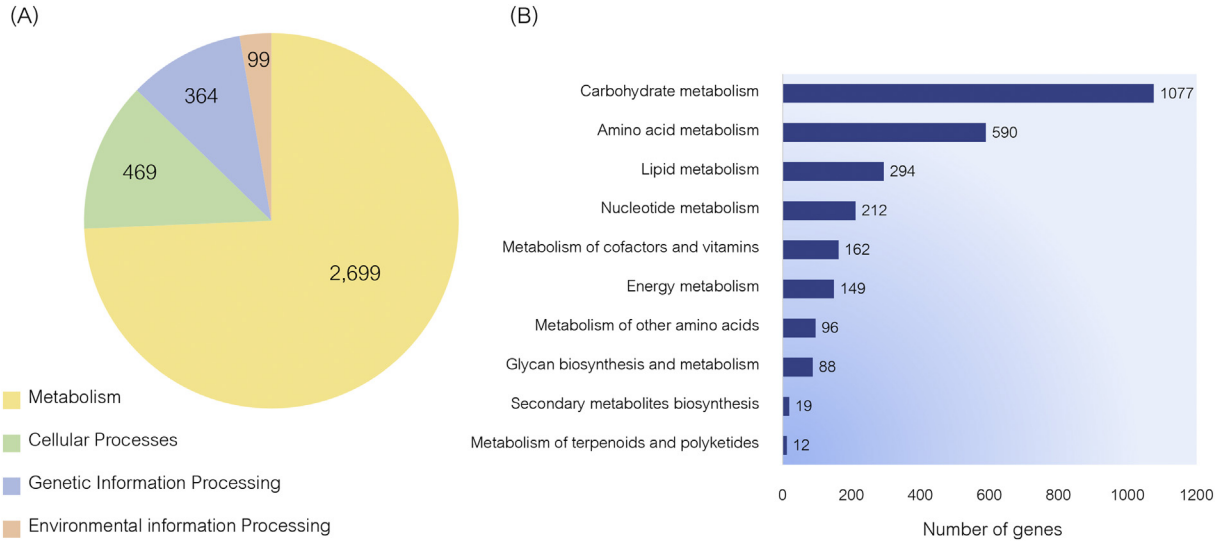

Fig. 3. Functional classification of significantly DEGs using KEGG annotation.

Table 3
List of significantly up-regulated genes of the xylose culture of *C. militaris* TBRC 7358.

Metabolisms Gene ID	EC number	Enzyme function
Amino acid metabolism		
Arginine and proline metabolism		
CL1812.Contig2	1.5.3.14	Polyamine oxidase
	1.5.99.6	Spermidine dehydrogenase
Histidine metabolism		
CL530.Contig2	3.4.13.18	N2-beta-alanylarginine dipeptidase
	3.4.13.20	beta-Ala-His dipeptidase
Tyrosine metabolism		
CL16.Contig2	4.1.2.52	4-hydroxy-2-oxoheptanedioate aldolase
Cysteine and methionine metabolism		
Unigene6255	3.5.99.7	1-aminocyclopropane-1-carboxylate aminohydrolase
Secondary metabolites biosynthesis		
Penicillin and cephalosporin biosynthesis		
Unigene2416	6.3.2.26	L-alpha-aminoadipyl-cysteinyl-valine
Aflatoxin biosynthesis		
Unigene2454	1.14.13.174	Averantin hydroxylase
Streptomycin biosynthesis		
CL131.Contig7	1.1.1.18	Inositol 2-dehydrogenase
Carbohydrate metabolism		
Fructose and mannose metabolism		
CL1376.Contig2	1.1.1.173	L-rhamnose 1-dehydrogenase
CL645.Contig1	1.1.1.14	Sorbitol dehydrogenase
	1.1.1.15	D-sorbitol dehydrogenase
Unigene5876	1.1.1.289	Sorbose reductase
Pentose and glucuronate interconversions		
CL1065.Contig1	2.7.1.17	D-xylulokinase
CL1065.Contig2		
CL1376.Contig3	1.1.1.372	Glyceraldehyde reductase
CL33.Contig2	1.1.1.9	D-xylulose reductase
Unigene5586	4.1.2.54	L-threo-3-deoxy-hexylosonate aldolase
Pentose phosphate pathway		
Unigene4068	3.1.1.17	Gluconolactonase
CL2305.Contig2	2.2.1.2	Dihydroxyacetonetransferase
Pyruvate metabolism		
CL171.Contig3	1.1.1.40	Malate dehydrogenase
Energy metabolism		
Nitrogen metabolism		
Unigene1105	1.13.12.16	Nitronate monooxygenase
Sulfur metabolism		
Unigene2321	1.14.14.5	Alkanesulfonate monooxygenase
Lipid metabolism		
Glycerolipid metabolism		
CL1376.Contig1	1.1.1.156	Glycerol 2-dehydrogenase
Cutin, suberine and wax biosynthesis		
Unigene2558	1.14.-.-	Oxygen oxidoreductase (22-hydroxylating)
Glycerophospholipid metabolism		
CL1234.Contig1	4.1.1.65	Phsophatidyl-L-serine carboxy-lyase
Sphingolipid metabolism		
CL640.Contig3	3.5.1.23	Acylsphingosine deacylase
Arachidonic acid metabolism		
Unigene840	5.3.99.5	Thromboxane synthase
Metabolism of cofactors and vitamins		
Pantothenate and CoA biosynthesis		
Unigene4892	1.1.1.169	2-dehydropantoate 2-reductase
Vitamin B6 metabolism		
Unigene5469	1.1.1.65	Pyridoxin dehydrogenase
Nucleotide metabolism		
Purine metabolism		
Unigene2635	6.3.4.4	Adenylosuccinate synthase

Note: The selected data were taken from the xylose culture with up-regulation of log2 fold change ≥ 1.5 and FDR ≤0.001 when compared with the glucose or sucrose cultures.

2.5. Validating transcriptome data using qRT-PCR

Expressions of a set of genes involved in the cordycepin biosynthesis and pentose and glucuronate interconversion of *C. militaris* cultures using different carbon sources were validated by qRT-PCR. Here, four genes (i.e. Unigene8329, Unigene902, Unigene2635, and Unigene5434) involved in cordycepin biosynthesis and two genes involved in pentose and glucuronate interconversion (i.e. CL1065.Contig2 and CL33.Contig2) were selected for gene expression validation. Expectedly, as a result of Table 5, the gene expression correlations between qRT-PCR (i.e. relative expression level) and RNA-seq data (i.e. FPKM value) of *C. militaris* cultures using different carbon sources are consistent.

3. Conclusion

In summary, *C. militaris* strain TBRC7358 was able to utilize a wide range of carbon sources for cell growth and cordycepin production. The differential expression of genes and the reporter metabolites analysis indicated a significant role of putative alternative routes in formation of precursors for cordycepin production on xylose. Not only for the transcription control by different carbon sources, but the metabolic response in cordycepin production also depended on the fungal strain. This study provides an insight in molecular mechanism in controlling the cordycepin biosynthesis in *C. militaris* that would be useful for either improving the cultivation process or the fungal strain for enhancement of biomass and cordycepin productivities as well as addressing biological means of the entomopathogenic fungal group.

4. Materials and methods

4.1. Fungal strain, cultivation process, and metabolite analysis

C. militaris strain TBRC7358 was used in this study. Cultivation processes were performed in 75 mL of defined medium [8] using xylose, sucrose and glucose as sole carbon sources. Samples were collected periodically and then filtered to separate the mycelial cells and fermented broth. For RNA extraction, the mycelial cells were harvested at logarithmic phases of the cultures (12, 14 and 30 days for the glucose, sucrose and xylose cultures, respectively) and immediately frozen by liquid nitrogen. The RNA samples were stored at −80 °C until further analysis.

For quantification of residual sugars and extracellular metabolites in fermented broth, the filtrates were determined by HPLC (Thermo Scientific, USA) on 300 mm × 7.8 mm (Aminex HPX−87H) column (Bio-Rad, USA). The column was eluted at 60 °C with 5 mmol/L H_2SO_4 using a flow rate of 0.6 mL/min, and metabolites were detected using RI detector. The results were analyzed by Chromeleon 7 (Ultimate 3000) software. The cordycepin concentration was measured by HPLC (Agilent, USA) on a HiQSil C18HS column (300 mm × 4.6 mm, 5 μm), maintained at 40 °C with 15% (*v*/v) methanol at a flow rate of 1.0 mL/min using UV detector with the wavelength of 260 nm.

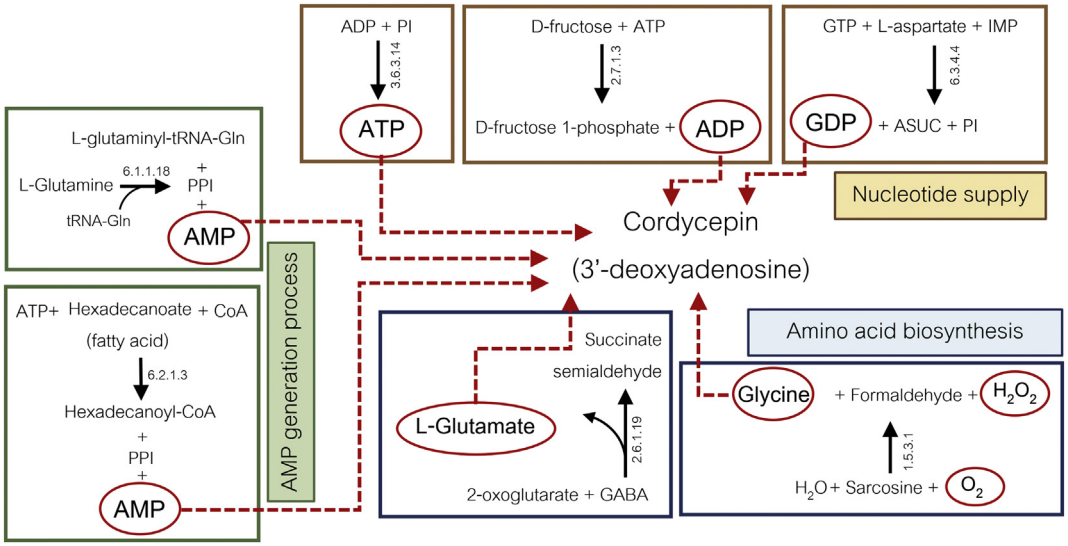

Fig. 4. Different metabolic routes of cordycepin biosynthesis starting from the precursor generation via AMP generation process, amino acid biosynthesis and nucleotide supply derived from reporter metabolites analysis. Note: the reporter metabolites are presented in red oval. The abbreviated metabolites are used as follows: ASUC (N6-(1,2-dicarboxyethyl)-AMP), PI (phosphate), PPI (pyrophosphate), and GABA (4-aminobutanoate). (For interpretation of the references to colour in this figure legend, the reader is referred to the web version of this article.)

4.2. RNA sequencing and de novo assembly

Total RNA of *C. militaris* strain TBRC7358 was extracted using the Qiagen RNeasy mini kit [28]. RNA quality and concentration were measured using an Agilent 2100 bioanalyzer and NanoDrop Spectrophotometer. After isolation of mRNA, the construction of the sequencing library and RNA sequencing were followed by Illumina HiSeq 4000. Clean reads were obtained by removing adapters, reads containing high content of unknown base (N) > 5% and the low quality reads (i.e. percentage of base was < 20% in a read). Trinity program [29] was used to perform de novo assembly with clean reads into longer contigs based on overlapping by the Inchworm module. RNA-Seq data was deposited in NCBI Sequence Read Archive (SRA) under bioproject PRJNA489225.

4.3. Transcriptome annotation and analysis

For transcriptome annotation and analysis, all transcripts derived from RNA-Seq data were annotated by searching against the KEGG database [14], EuKaryotic Orthologous Groups (KOG) [30] and non-redundant protein sequence database (NR) using BLASTX [31] with an *E*-value of 1E-05 [32]. In addition, the annotated data of *C. militaris* strain TBRC6039 [8] and *C. militaris* strain CM01 [10] were also used for functional annotation by BLASTN and BLASTX, respectively with an E-value of 1E-50 using the Bidirectional Best Hit method (BBH) with 1:1 orthologs. Apart from sequencing interpretation, the relative expression

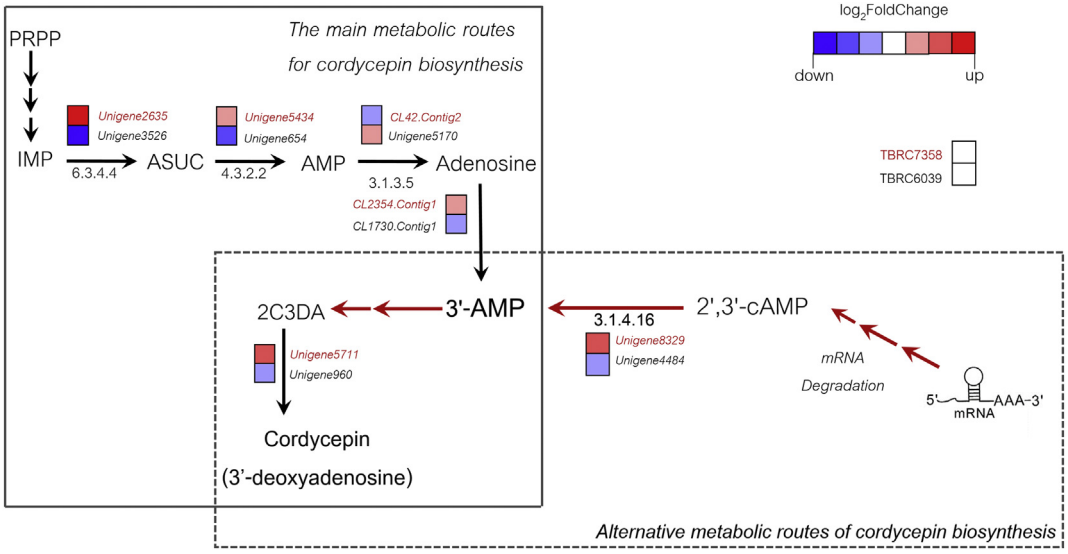

Fig. 5. A putative metabolic routes towards 3′-AMP formation in relation to cordycepin biosynthesis of *C. militaris* strain TBRC7358 when compared to the reference strain TBRC6039. Note: A value of log2 fold change was selected from a comparison of xylose and glucose cultures. A black arrow means the main metabolic routes associated in adenosine via 3′-AMP formation through cordycepin biosynthesis. A red arrow represents putative alternative metabolic routes through 3′-AMP-associated cordycepin biosynthesis. The templates of metabolic routes were taken from the previous reports [8,11,12]. The abbreviated metabolites are used as follows: PRPP (phosphoribosyl pyrophosphate), ASUC (N6-(1,2-dicarboxyethyl)-AMP), AMP (adenosine-5′-monophosphate), 2′,3′-cAMP (2′3′-cyclic monophosphate), 3′-AMP (adenosine-3′-monophosphate), and 2C3DA (2′-carbonyl-3′-deoxyadenosine). (For interpretation of the references to colour in this figure legend, the reader is referred to the web version of this article.)

Table 4
List of the expressed genes involved in cordycepin biosynthetic routes comparing between *C. militaris* strain TBRC7358 and reference strain TBRC6039.

EC-number	Enzyme function	TBRC7358	TBRC6039	Fold
		Gene ID	Gene ID	Change
3.1.4.16	2′,3′-cyclic-nucleotide 2′-phosphodiesterase	Unigene8329	Unigene4484	2.85
		Unigene6827	–	–
2.7.7.72	CCA tRNA nucleotidyltransferase	Unigene902	Unigene7018	2.82
–	Oxidoreductase domain-containing protein (2′-carbonyl-3′-deoxyadenosine)	Unigene5711	Unigene960	1.9
6.3.4.4	Adenylosuccinate synthase	Unigene2635	Unigene3526	31.88
4.3.2.2	Adenylosuccinate lyase	Unigene5434	Unigene654	1.22
3.1.3.5	5′-nucleotidase	CL42.Contig2	Unigene5170	0.55
2.7.4.3	Adenylate kinase	CL794.Contig3	CL1509.Contig2	3.39
		Unigene2245	Unigene5848	0.68
		Unigene2885	Unigene2082	0.69
2.7.1.20	Adenosine kinase	CL1742.Contig2	CL1994.Contig2	1.54
2.7.4.6	Nucleoside-diphosphate kinase	Unigene1364	CL1038.Contig2	1.59
3.4.11.1	Leucyl aminopeptidase	CL44.Contig1	CL1285.Contig1	6.16
2.6.1.42	Branched-chain-amino-acid transaminase	CL1066.Contig1	CL1243.Contig4	2.33
2.4.2.17	ATP phosphoribosyltransferase	Unigene6275	Unigene2403	1.96
		CL2354.Contig2	CL1730.Contig2	0.70
		CL2354.Contig1	CL1730.Contig1	0.73

Note: The selected data were taken from the xylose cultures of *C. militaris* between the strain TBRC7358 and the reference strain (TBRC6039). A fold change of the transcript levels between the two strains was calculated by dividing FPKM value of orthologous genes of interest of the strain TBRC7358 to the strain TBRC6039 [8].

abundances in the form of fragments per kilobase of transcript per million mapped reads (FPKM) were calculated for all transcripts. Here, FPKM value ≥1 meant all transcripts with expression. For DEGs analysis, false discovery rate (FDR) ≤0.001 was set as a threshold for gaining significantly DEGs across different carbon sources.

4.4. Reporter metabolites analysis

The reporter metabolites algorithm was applied as described by Patil and Nielsen, 2005 [21]. The analysis was performed for a pairwise carbon sources comparison (i.e. xylose to other carbon sources). For this purpose, information on the topology of the constructed metabolic network of *C. militaris* [11] in conjunction with the FDR value, referring DEGs of the *C. militaris* strain TBRC7358 across different carbon sources were used.

4.5. Comparative transcriptome analysis between C. militaris strains

To distinguish the transcriptional response between *C. militaris* strains, the transcriptome data of the strain TBRC7358 was compared with the previously published data of the reference strain (TBRC6039), which were derived from the 14-day sucrose, 16-day glucose and 45-day xylose cultures under the same cultivation condition [8]. A fold change of the transcripts between the two strains grown at the logarithmic phases was calculated by dividing FPKM value of orthologous genes of interest of the strain TBRC7358 to the reference strain TBRC6039.

4.6. Gene expression analysis using qRT-PCR

Expressions of a set of selected genes of *C. militaris* cultures using different carbon sources were validated by qRT-PCR. Total RNA of *C. militaris* was extracted using RNeasy mini kit (Qiagen), and then

Table 5
qRT-PCR analysis of the significantly up-regulated genes involved in the cordycepin biosynthesis, and pentose and glucuronate interconversion of *C. militaris* strain TBRC7358.

Gene ID	Enzyme function	EC number	Carbon sources	Relative* expression level (fold)	Gene expression level (FPKM value)
Cordycepin biosynthesis					
Unigene8329	2′,3′-cyclic-nucleotide 2′-phosphodiesterase	3.1.4.16	Glucose	1.00 ± 1.65^{b}	0.91
			Sucrose	1.13 ± 0.71^{b}	0.68
			Xylose	3.21 ± 0.43^{a}	5.38
Unigene902	CCA tRNA nucleotidyltransferase	2.7.7.72	Glucose	1.00 ± 0.36^{b}	4.73
			Sucrose	0.66 ± 0.06^{b}	5.08
			Xylose	2.01 ± 0.14^{a}	10.45
Unigene2635	Adenylosuccinate synthase	6.3.4.4	Glucose	1.00 ± 0.37^{c}	5.78
			Sucrose	3.04 ± 0.30^{b}	6.12
			Xylose	9.50 ± 0.70^{a}	126.87
Unigene5434	Adenylosuccinate lyase	4.3.2.2	Glucose	1.00 ± 0.26^{b}	395.42
			Sucrose	1.82 ± 0.44^{a}	338.12
			Xylose	1.29 ± 1.16^{a,b}	409.44
Pentose and glucuronate interconversion					
CL1065.Contig2	D-xylulokinase	2.7.1.17	Glucose	1.00 ± 0.34^{b}	14.83
			Sucrose	0.64 ± 0.08^{b}	15.56
			Xylose	1.62 ± 0.23^{a}	58.62
CL33.Contig2	D-xylulose reductase	1.1.1.9	Glucose	1.00 ± 1.05^{b}	14.88
			Sucrose	4.30 ± 0.90^{a}	25.29
			Xylose	5.66 ± 0.46^{a}	311.69

a,b,c Different upper-case letters indicate statistically significant differences in each gene (P ≤ .05, Tukey's test) among the cultures using different carbon sources.
* Values of relative expression levels (fold) were calculated by using the glucose culture as a control set. The presented value shows as means ± SD.

reverse-transcribed using RevertAid First Strand cDNA Synthesis Kit (Thermo Scientific, Lithuania). qRT-PCR was performed using Ssoadvanced™ Universal SYBR® Green Supermix (Bio-Rad, USA) with a CFX96 Touch Real-Time PCR System (Bio-Rad, USA). The primers specific to the targeted gene sequences are shown in Supplementary file 6. The actin gene of *C. militaris* was used as normalization reference for the gene expression values. The reaction cycling conditions were as follows: 95 °C for 30 s, followed by 39 cycles at 95 °C for 10 s, and 60 °C for 30 s. Melt curves were obtained by increasing the temperature from 65 °C to 95 °C with increments of 0.5 °C per 5 s. Three biological replicates were performed for individual sample. The quantitation cycle (Cq) value from qRT-PCR was used to calculate relative expression levels by the $2^{-\Delta\Delta Ct}$ method [33].

(A) The pie chart shows the number of genes in each of four major functional categories. (B) The bar chart shows the number of genes devoted to different categories of metabolism.

Supplementary data to this article can be found online at https://doi.org/10.1016/j.ygeno.2019.04.015.

Acknowledgements

This work was supported by The Thailand Research Fund (RSA6180001), National Research Council of Thailand (NRCT) and Department of Zoology, Faculty of Science, Kasetsart University. BW gratefully acknowledges financial support from Faculty of Science Kasetsart University Postgraduate Studentship (ScKUPGS) at Kasetsart University and NRCT grant. N.R acknowledges financial support from Science Achievement Scholarship of Thailand (SAST), the International Affairs Division (IAD) at Kasetsart University and NRCT grant. W·V would like to thank Omics Center for Agriculture, Bioresources, Food, and Health, Faculty of Science, Kasetsart University (OmiKU). The authors also would like to thank Computational Biomodelling Laboratory for Agricultural Science and Technology (CBLAST), Faculty of Science, Kasetsart University for computing facilities and resources. We are grateful to Ms. Jutamas Anatayanon, BIOTEC, for technical assistance in qRT-PCR analysis.

Author contributions statement

B.W performed experiments, analyzed the data, wrote the main manuscript, N.R carried out the data analysis and interpretation. W.V and K.L interpreted and discussed the results, wrote and revised the manuscript. P.C and J.W guided the experimental design and data analysis. W.V conceived, designed all experiments and supervised throughout the study. All authors reviewed and approved the final manuscript.

Competing financial interests

The authors declare no competing financial interests.

Data accessibility

Raw Illumina HiSeq 4000 sequences have been deposited to NCBI Sequence Read Archive (SRA) under the BioProject accession number PRJNA489225.

References

[1] J.M. Park, J.S. Lee, K.R. Lee, S.J. Ha, E.K. Hong, *Cordyceps militaris* extract protects human dermal fibroblasts against oxidative stress-induced apoptosis and premature senescence, Nutrients 6 (2014) 3711–3726.

[2] J. Yin, X. Xin, Y. Weng, Z. Gui, Transcriptome-wide analysis reveals the progress of *Cordyceps militaris* subculture degeneration, PLoS One 12 (2017) e0186279.

[3] L.T. Lin, Y.J. Lai, S.C. Wu, W.H. Hsu, C.J. Tai, Optimal conditions for cordycepin production in surface liquid-cultured *Cordyceps militaris* treated with porcine liver extracts for suppression of oral cancer, J. Food Drug Anal. 26 (2018) 135–144.

[4] M. Masuda, E. Urabe, A. Sakurai, M. Sakakibara, Production of cordycepin by surface culture using the medicinal mushroom *Cordyceps militaris*, Enzym. Microb. Technol. 39 (2006) 641–646.

[5] I.L. Shih, K.-L. Tsai, C. Hsieh, Effects of culture conditions on the mycelial growth and bioactive metabolite production in submerged culture of *Cordyceps militaris*, Biochem. Eng. J. 33 (2007) 193–201.

[6] T. Jiapeng, L. Yiting, Z. Li, Optimization of fermentation conditions and purification of cordycepin from *Cordyceps militaris*, Prep. Biochem. Biotechnol. 44 (2014) 90–106.

[7] X.B. Mao, T. Eksriwong, S. Chauvatcharin, J.J. Zhong, Optimization of carbon source and carbon/nitrogen ratio for cordycepin production by submerged cultivation of medicinal mushroom *Cordyceps militaris*, Process Biochem. 40 (2005) 1667–1672.

[8] N. Raethong, K. Laoteng, W. Vongsangnak, Uncovering global metabolic response to cordycepin production in *Cordyceps militaris* through transcriptome and genome-scale network-driven analysis, Sci. Rep. 8 (2018) 9250.

[9] C. Kang, T.C. Wen, J.C. Kang, Z.B. Meng, G.R. Li, K.D. Hyde, Optimization of large-scale culture conditions for the production of cordycepin with *Cordyceps militaris* by liquid static culture, Sci. World J. 2014 (2014) 510627.

[10] P. Zheng, Y. Xia, G. Xiao, C. Xiong, X. Hu, S. Zhang, H. Zheng, Y. Huang, Y. Zhou, S. Wang, G.P. Zhao, X. Liu, R.J.S. Leger, C. Wang, Genome sequence of the insect pathogenic fungus *Cordyceps militaris*, a valued traditional chinese medicine, Genome Biol. 12 (2011) R116.

[11] W. Vongsangnak, N. Raethong, W. Mujchariyakul, N.N. Nguyen, H.W. Leong, K. Laoteng, Genome-scale metabolic network of *Cordyceps militaris* useful for comparative analysis of entomopathogenic fungi, Gene 626 (2017) 132–139.

[12] Y. Xia, F. Luo, Y. Shang, P. Chen, Y. Lu, C. Wang, Fungal cordycepin biosynthesis is coupled with the production of the safeguard molecule pentostatin, Cell Chem. Biol. 24 (2017) 1479–1489.

[13] X.B. Mao, J.J. Zhong, Hyperproduction of Cordycepin by two-stage dissolved oxygen control in submerged cultivation of medicinal mushroom *Cordyceps militaris* in bioreactors, Biotechnol. Prog. 20 (2004) 1408–1413.

[14] M. Kanehisa, S. Goto, S. Kawashima, Y. Okuno, M. Hattori, The KEGG resource for deciphering the genome, Nucleic Acids Res. 32 (2004) D277–D280.

[15] M. Klein, S. Swinnen, J.M. Thevelein, E. Nevoigt, Glycerol metabolism and transport in yeast and fungi: established knowledge and ambiguities, Environ. Microbiol. 19 (2017) 878–893.

[16] M.J. de Groot, W. Prathumpai, J. Visser, G.J. Ruijter, Metabolic control analysis of *Aspergillus niger* L-arabinose catabolism, Biotechnol. Prog. 21 (2005) 1610–1616.

[17] O.M. Koivistoinen, S. Hilditch, S.P. Voutilainen, H. Boer, M. Penttila, P. Richard, Identification in the yeast *Pichia stipitis* of the first L-rhamnose-1-dehydrogenase gene, FEBS J. 275 (2008) 2482–2488.

[18] A.P.J. Trinci, A. Collinge, Influence of L-sorbose on the growth and morphology of *Neurospora crassa*, J. Gen. Microbiol. 78 (1973) 179–192.

[19] Y. Yin, G. Yu, Y. Chen, S. Jiang, M. Wang, Y. Jin, X. Lan, Y. Liang, H. Sun, Genome-wide transcriptome and proteome analysis on different developmental stages of *Cordyceps militaris*, PLoS One 7 (2012) e51853.

[20] F. Pang, L. Wang, Y. Jin, L. Guo, L. Song, G. Liu, C. Feng, Transcriptome analysis of *Paecilomyces hepiali* at different growth stages and culture additives to reveal putative genes in cordycepin biosynthesis, Genomics 110 (2018) 162–170.

[21] K.R. Patil, J. Nielsen, Uncovering transcriptional regulation of metabolism by using metabolic network topology, Proc. Natl. Acad. Sci. U. S. A. 102 (2005) 2685–2689.

[22] A. Suparmin, T. Kato, H. Dohra, E.Y. Park, Insight into cordycepin biosynthesis of *Cordyceps militaris*: comparison between a liquid surface culture and a submerged culture through transcriptomic analysis, PLoS One 12 (2017) e0187052.

[23] J.C. Nielsen, J. Nielsen, Development of fungal cell factories for the production of secondary metabolites: linking genomics and metabolism, Synth. Syst. Biotechnol. 2 (2017) 5–12.

[24] Q. Zhang, Y. Liu, The strategies for increasing cordycepin production of *Cordyceps militaris* by liquid fermentation, Fungal. Genom. Biol. 6 (1) (2016).

[25] A.F. Yakunin, M. Proudfoot, E. Kuznetsova, A. Savchenko, G. Brown, C.H. Arrowsmith, A.M. Edwards, The HD domain of the *Escherichia coli* tRNA nucleotidyltransferase has 2′,3′-cyclic phosphodiesterase, 2′-nucleotidase, and phosphatase activities, J. Biol. Chem. 279 (2004) 36819–36827.

[26] E.K. Jackson, J. Ren, Z. Mi, Extracellular 2′,3′-cAMP is a source of adenosine, J. Biol. Chem. 284 (2009) 33097–33106.

[27] Y. Xiong, T.A. Steitz, A story with a good ending: tRNA 3′-end maturation by CCA-adding enzymes, Curr. Opin. Struct. Biol. 16 (2006) 12–17.

[28] G.M. Leite, N. Magan, A. Medina, Comparison of different bead-beating RNA extraction strategies: an optimized method for filamentous fungi, J. Microbiol. Methods 88 (2012) 413–418.

[29] M.L. Holding, M.J. Margres, A.J. Mason, C.L. Parkinson, D.R. Rokyta, Evaluating the performance of *de novo* assembly methods for venom-gland transcriptomics, Toxins (Basel) 10 (2018) 249.

[30] H.Y. Song, D.H. Kim, J.M. Kim, Comparative transcriptome analysis of dikaryotic mycelia and mature fruiting bodies in the edible mushroom Lentinula edodes, Sci. Rep. 8 (2018) 8983.

[31] K. Nurul, H. Shibuya, T. Kikuchi, Analysis of expressed sequence tags from the wood-decaying fungus *Fomitopsis palustris* and identification of potential genes involved in the decay process, J. Microbiol. Biotechnol. 21 (2011) 347–358.

[32] S. Sinha, S. Flibotte, M. Neira, S. Formby, A. Plemenitas, N.G. Cimerman, M. Lenassi, C. Gostincar, J.E. Stajich, C. Nislow, Insight into the recent genome duplication of the halophilic yeast *Hortaea*: combining an improved genome with gene expression and chromatin structure, G3 (Bethesda) 7 (2017) 2015–2022.

[33] K.J. Livak, T.D. Schmittgen, Analysis of relative gene expression data using real-time quantitative PCR and the 2-ΔΔCt, Methods 25 (2001) 402–408.